



- C. Royon,<sup>18</sup> P. Rubinov,<sup>50</sup> R. Ruchti,<sup>55</sup> G. Safronov,<sup>37</sup> G. Sajot,<sup>14</sup> A. Sánchez-Hernández,<sup>33</sup> M. P. Sanders,<sup>17</sup> B. Sanghi,<sup>50</sup>  
 G. Savage,<sup>50</sup> L. Sawyer,<sup>60</sup> T. Scanlon,<sup>43</sup> D. Schaile,<sup>25</sup> R. D. Schamberger,<sup>72</sup> Y. Scheglov,<sup>40</sup> H. Schellman,<sup>53</sup>  
 T. Schliephake,<sup>26</sup> S. Schlobohm,<sup>82</sup> C. Schwanenberger,<sup>44</sup> A. Schwartzman,<sup>68</sup> R. Schwienhorst,<sup>65</sup> J. Sekaric,<sup>49</sup>  
 H. Severini,<sup>75</sup> E. Shabalina,<sup>51</sup> M. Shamim,<sup>59</sup> V. Shary,<sup>18</sup> A. A. Shchukin,<sup>39</sup> R. K. Shivpuri,<sup>28</sup> V. Siccardi,<sup>19</sup> V. Simak,<sup>10</sup>  
 V. Sirotenko,<sup>50</sup> P. Skubic,<sup>75</sup> P. Slattery,<sup>71</sup> D. Smirnov,<sup>55</sup> G. R. Snow,<sup>67</sup> J. Snow,<sup>74</sup> S. Snyder,<sup>73</sup> S. Söldner-Rembold,<sup>44</sup>  
 L. Sonnenschein,<sup>17</sup> A. Sopczak,<sup>42</sup> M. Sosebee,<sup>78</sup> K. Soustruznik,<sup>9</sup> B. Spurlock,<sup>78</sup> J. Stark,<sup>14</sup> J. Steele,<sup>60</sup> V. Stolin,<sup>37</sup>  
 D. A. Stoyanova,<sup>39</sup> J. Strandberg,<sup>64</sup> S. Strandberg,<sup>41</sup> M. A. Strang,<sup>69</sup> E. Strauss,<sup>72</sup> M. Strauss,<sup>75</sup> R. Ströhmer,<sup>25</sup> D. Strom,<sup>53</sup>  
 L. Stutte,<sup>50</sup> S. Sumowidagdo,<sup>49</sup> P. Svoisky,<sup>55</sup> A. Sznajder,<sup>3</sup> P. Tamburello,<sup>45</sup> A. Tanasijczuk,<sup>1</sup> W. Taylor,<sup>6</sup> B. Tiller,<sup>25</sup>  
 F. Tissandier,<sup>13</sup> M. Titov,<sup>18</sup> V. V. Tokmenin,<sup>36</sup> I. Torchiani,<sup>23</sup> D. Tsbychev,<sup>72</sup> B. Tuchming,<sup>18</sup> C. Tully,<sup>68</sup> P. M. Tuts,<sup>70</sup>  
 R. Unalan,<sup>65</sup> L. Uvarov,<sup>40</sup> S. Uvarov,<sup>40</sup> S. Uzunyan,<sup>52</sup> B. Vachon,<sup>6</sup> P. J. van den Berg,<sup>34</sup> R. Van Kooten,<sup>54</sup>  
 W. M. van Leeuwen,<sup>34</sup> N. Varelas,<sup>51</sup> E. W. Varnes,<sup>45</sup> I. A. Vasilyev,<sup>39</sup> P. Verdier,<sup>20</sup> L. S. Vertogradov,<sup>36</sup> M. Verzocchi,<sup>50</sup>  
 D. Vilanova,<sup>18</sup> F. Villeneuve-Seguier,<sup>43</sup> P. Vint,<sup>43</sup> P. Vokac,<sup>10</sup> M. Voutilainen,<sup>67</sup><sup>II</sup> R. Wagner,<sup>68</sup> H. D. Wahl,<sup>49</sup>  
 M. H. L. S. Wang,<sup>50</sup> J. Warchol,<sup>55</sup> G. Watts,<sup>82</sup> M. Wayne,<sup>55</sup> G. Weber,<sup>24</sup> M. Weber,<sup>50</sup><sup>III</sup> L. Welty-Rieger,<sup>54</sup> A. Wenger,<sup>23,\*\*</sup>  
 N. Wermes,<sup>22</sup> M. Wetstein,<sup>61</sup> A. White,<sup>78</sup> D. Wicke,<sup>26</sup> M. Williams,<sup>42</sup> G. W. Wilson,<sup>58</sup> S. J. Wimpenny,<sup>48</sup> M. Wobisch,<sup>60</sup>  
 D. R. Wood,<sup>63</sup> T. R. Wyatt,<sup>44</sup> Y. Xie,<sup>77</sup> S. Yacoob,<sup>53</sup> R. Yamada,<sup>50</sup> W.-C. Yang,<sup>44</sup> T. Yasuda,<sup>50</sup> Y. A. Yatsunenko,<sup>36</sup> H. Yin,<sup>7</sup>  
 K. Yip,<sup>73</sup> H. D. Yoo,<sup>77</sup> S. W. Youn,<sup>53</sup> J. Yu,<sup>78</sup> C. Zeitnitz,<sup>26</sup> S. Zelitch,<sup>81</sup> T. Zhao,<sup>82</sup> B. Zhou,<sup>64</sup> J. Zhu,<sup>72</sup> M. Zielinski,<sup>71</sup>  
 D. Zieminska,<sup>54</sup> A. Zieminski,<sup>54</sup><sup>††</sup> L. Zivkovic,<sup>70</sup> V. Zutshi,<sup>52</sup> and E. G. Zverev<sup>38</sup>

(D0 Collaboration)

<sup>1</sup>Universidad de Buenos Aires, Buenos Aires, Argentina<sup>2</sup>LAFEX, Centro Brasileiro de Pesquisas Físicas, Rio de Janeiro, Brazil<sup>3</sup>Universidade do Estado do Rio de Janeiro, Rio de Janeiro, Brazil<sup>4</sup>Universidade Federal do ABC, Santo André, Brazil<sup>5</sup>Instituto de Física Teórica, Universidade Estadual Paulista, São Paulo, Brazil<sup>6</sup>University of Alberta, Edmonton, Alberta, Canada,

Simon Fraser University, Burnaby, British Columbia, Canada,

York University, Toronto, Ontario, Canada,

and McGill University, Montreal, Quebec, Canada

<sup>7</sup>University of Science and Technology of China, Hefei, People's Republic of China<sup>8</sup>Universidad de los Andes, Bogotá, Colombia<sup>9</sup>Center for Particle Physics, Charles University, Prague, Czech Republic<sup>10</sup>Czech Technical University, Prague, Czech Republic<sup>11</sup>Center for Particle Physics, Institute of Physics, Academy of Sciences of the Czech Republic, Prague, Czech Republic<sup>12</sup>Universidad San Francisco de Quito, Quito, Ecuador<sup>13</sup>LPC, Université Blaise Pascal, CNRS/IN2P3, Clermont, France<sup>15</sup>CPPM, Aix-Marseille Université, CNRS/IN2P3, Marseille, France<sup>16</sup>LAL, Université Paris-Sud, IN2P3/CNRS, Orsay, France<sup>17</sup>LPNHE, IN2P3/CNRS, Universités Paris VI and VII, Paris, France<sup>18</sup>CEA, Ifju, SPP, Saclay, France<sup>19</sup>IPHC, Université Louis Pasteur, CNRS/IN2P3, Strasbourg, France<sup>20</sup>IPNL, Université Lyon 1, CNRS/IN2P3, Villeurbanne, France and Université de Lyon, Lyon, France<sup>21</sup>III. Physikalisches Institut A, RWTH Aachen University, Aachen, Germany<sup>22</sup>Physikalisches Institut, Universität Bonn, Bonn, Germany<sup>23</sup>Physikalisches Institut, Universität Freiburg, Freiburg, Germany<sup>24</sup>Institut für Physik, Universität Mainz, Mainz, Germany<sup>25</sup>Ludwig-Maximilians-Universität München, München, Germany<sup>26</sup>Fachbereich Physik, University of Wuppertal, Wuppertal, Germany<sup>27</sup>Panjab University, Chandigarh, India<sup>28</sup>Delhi University, Delhi, India<sup>29</sup>Tata Institute of Fundamental Research, Mumbai, India<sup>30</sup>University College Dublin, Dublin, Ireland<sup>31</sup>Korea Detector Laboratory, Korea University, Seoul, Korea<sup>32</sup>SungKyunKwan University, Suwon, Korea<sup>33</sup>CINVESTAV, Mexico City, Mexico<sup>34</sup>FOM-Institute NIKHEF and University of Amsterdam/NIKHEF, Amsterdam, The Netherlands

<sup>35</sup>Radboud University Nijmegen/NIKHEF, Nijmegen, The Netherlands<sup>36</sup>Joint Institute for Nuclear Research, Dubna, Russia<sup>37</sup>Institute for Theoretical and Experimental Physics, Moscow, Russia<sup>38</sup>Moscow State University, Moscow, Russia<sup>39</sup>Institute for High Energy Physics, Protvino, Russia<sup>40</sup>Petersburg Nuclear Physics Institute, St. Petersburg, Russia<sup>41</sup>Lund University, Lund, Sweden, Royal Institute of Technology and Stockholm University, Stockholm, Sweden, and Uppsala University, Uppsala, Sweden<sup>42</sup>Lancaster University, Lancaster, United Kingdom<sup>43</sup>Imperial College, London, United Kingdom<sup>44</sup>University of Manchester, Manchester, United Kingdom<sup>45</sup>University of Arizona, Tucson, Arizona 85721, USA<sup>46</sup>Lawrence Berkeley National Laboratory and University of California, Berkeley, California 94720, USA<sup>47</sup>California State University, Fresno, California 93740, USA<sup>48</sup>University of California, Riverside, California 92521, USA<sup>49</sup>Florida State University, Tallahassee, Florida 32306, USA<sup>50</sup>Fermi National Accelerator Laboratory, Batavia, Illinois 60510, USA<sup>51</sup>University of Illinois at Chicago, Chicago, Illinois 60607, USA<sup>52</sup>Northern Illinois University, DeKalb, Illinois 60115, USA<sup>53</sup>Northwestern University, Evanston, Illinois 60208, USA<sup>54</sup>Indiana University, Bloomington, Indiana 47405, USA<sup>55</sup>University of Notre Dame, Notre Dame, Indiana 46556, USA<sup>56</sup>Purdue University Calumet, Hammond, Indiana 46323, USA<sup>57</sup>Iowa State University, Ames, Iowa 50011, USA<sup>58</sup>University of Kansas, Lawrence, Kansas 66045, USA<sup>59</sup>Kansas State University, Manhattan, Kansas 66506, USA<sup>60</sup>Louisiana Tech University, Ruston, Louisiana 71272, USA<sup>61</sup>University of Maryland, College Park, Maryland 20742, USA<sup>62</sup>Boston University, Boston, Massachusetts 02215, USA<sup>63</sup>Northeastern University, Boston, Massachusetts 02115, USA<sup>64</sup>University of Michigan, Ann Arbor, Michigan 48109, USA<sup>65</sup>Michigan State University, East Lansing, Michigan 48824, USA<sup>66</sup>University of Mississippi, University, Mississippi 38677, USA<sup>67</sup>University of Nebraska, Lincoln, Nebraska 68588, USA<sup>68</sup>Princeton University, Princeton, New Jersey 08544, USA<sup>69</sup>State University of New York, Buffalo, New York 14260, USA<sup>70</sup>Columbia University, New York, New York 10027, USA<sup>71</sup>University of Rochester, Rochester, New York 14627, USA<sup>72</sup>State University of New York, Stony Brook, New York 11794, USA<sup>73</sup>Brookhaven National Laboratory, Upton, New York 11973, USA<sup>74</sup>Langston University, Langston, Oklahoma 73050, USA<sup>75</sup>University of Oklahoma, Norman, Oklahoma 73019, USA<sup>76</sup>Oklahoma State University, Stillwater, Oklahoma 74078, USA<sup>77</sup>Brown University, Providence, Rhode Island 02912, USA<sup>78</sup>University of Texas, Arlington, Texas 76019, USA<sup>79</sup>Southern Methodist University, Dallas, Texas 75275, USA<sup>80</sup>Rice University, Houston, Texas 77005, USA<sup>81</sup>University of Virginia, Charlottesville, Virginia 22901, USA<sup>82</sup>University of Washington, Seattle, Washington 98195, USA

(Received 14 August 2008; published 4 February 2009)

We present results of a search for  $WH \rightarrow \ell\nu b\bar{b}$  production in  $p\bar{p}$  collisions based on the analysis of  $1.05 \text{ fb}^{-1}$  of data collected by the D0 experiment at the Fermilab Tevatron, using a neural network for separating the signal from backgrounds. No signal-like excess is observed, and we set 95% C.L. upper limits on the  $WH$  production cross section multiplied by the branching ratio for  $H \rightarrow b\bar{b}$  for Higgs boson masses between 100 and 150 GeV. For a mass of 115 GeV, we obtain an observed (expected) limit of 1.5 (1.4) pb, a factor of 11.4 (10.7) times larger than the standard model prediction.

The Higgs boson is the last unobserved particle of the standard model (SM). As a remnant of spontaneous electroweak symmetry breaking, it is fundamentally different from the other elementary particles, and its observation would support the hypothesis that the Higgs mechanism generates the masses of the weak gauge bosons and the charged fermions. The Higgs boson mass ( $m_H$ ) is not theoretically predicted, but the combination of results from direct searches at the CERN LEP collider [1] with the indirect constraints from precision electroweak measurements results in a preferred range of  $114.4 < m_H < 185$  GeV at 95% C.L. [2]. Such a mass range can be probed at the Fermilab Tevatron collider. In this Letter, we concentrate on the most sensitive production channel at the Tevatron for Higgs bosons of mass below 125 GeV, i.e., the associated production of a Higgs boson with a  $W$  boson. Several searches for  $WH$  production have been published at a center-of-mass energy of  $\sqrt{s} = 1.96$  TeV. Two [3,4] used subsamples (0.17 and  $0.44 \text{ fb}^{-1}$ ) of the data reported in this Letter, while two others, from the CDF Collaboration, are based on  $0.32$  and  $0.95 \text{ fb}^{-1}$  of integrated luminosity [5,6].

This analysis uses  $1.05 \text{ fb}^{-1}$  of D0 [7,8] data, collected between April 2002 and February 2006. As in our previous  $WH$  analyses [3,4], we require one high transverse momentum ( $p_T$ ) lepton ( $e$  or  $\mu$ ) and missing transverse energy  $\cancel{E}_T$  to account for the neutrino from the  $W$  boson decay, and two jets from the decay of the Higgs boson, with at least one of them being identified as originating from a bottom ( $b$ ) quark jet. We extend this data selection by including also events with three jets and events with “forward” electrons detected at pseudorapidities [9]  $|\eta| > 1.5$ . We also now accept the small contribution originating from misreconstructed  $ZH$ , in which only one lepton from the  $Z$  is identified. In addition, we use a more inclusive trigger selection in the muon channel, increasing the detection efficiency from approximately 70% to 100% [10], we improve the  $b$ -jet identification using a neural network algorithm [11], and we enhance the signal to background discrimination using a neural network for the  $W + 2$  jet events. Overall, the improvements in analysis techniques have led to an increase of about 40% in the sensitivity (for an equivalent luminosity) to a Higgs boson with mass 115 GeV, with respect to our previous analysis [4].

For the  $e$  channel, the  $W +$  jets candidate events are collected, with  $\approx 90\%$  efficiency, by triggers that require at least one electromagnetic object in the calorimeter. In the  $\mu$  channel,  $\approx 90\%$  of the candidates are collected by triggers requiring a single muon or a muon plus a jet, while the remaining 10% of events are collected by other triggers, for a total trigger efficiency of  $\approx 100\%$ , as estimated in data [10].

The event selection requires one lepton candidate with  $p_T > 15$  GeV,  $\cancel{E}_T > 20$  GeV ( $\cancel{E}_T > 25$  GeV for events with a forward electron), and exactly two jets with  $p_T >$

25 and 20 GeV, and  $|\eta| < 2.5$ , or exactly three jets with  $p_T > 25, 20$ , and 20 GeV, and  $|\eta| < 2.5$ . We also require the scalar sum of the  $p_T$  of the jets to be  $> 60$  GeV, the  $W$  transverse mass  $M_W^T$  reconstructed from the  $\cancel{E}_T$ , and the lepton  $p_T$  to be greater than  $40$  GeV  $- 0.5 \times \cancel{E}_T$  to reject multijet background, and the primary interaction vertex to take place within the longitudinal acceptance of the vertex detector. Jets are reconstructed using a midpoint cone algorithm [12] with a radius of 0.5. The  $\cancel{E}_T$  is calculated from energies in calorimeter cells and corrected for the  $p_T$  of identified muons. All energy corrections applied to electrons or jets are also propagated to the  $\cancel{E}_T$ .

A central (forward) electron is required to have  $|\eta| < 1.1$  ( $1.5 < |\eta| < 2.5$ ). To reject fake electrons originating mostly from instrumental effects (track-photon overlap), the electron candidates must satisfy two sets of identification (“loose” and “tight”) criteria [4]. The efficiencies of these requirements are determined from a pure sample of  $Z \rightarrow e^+ e^-$  events. The differential multijet background for every relevant distribution is then estimated from the loose and tight lepton samples [4,13]. The same statistical method is used for muons but with different loose or tight definitions. Muons are reconstructed using information from the outer muon detector and the central tracker and must have  $|\eta| < 2.0$ . To reject muons originating from semileptonic decays of heavy-flavor hadrons, we exploit the fact that they have lower  $p_T$  than those originating from  $W$  decay and are generally not isolated because of accompanying jet fragments. The loose isolation criterion is thus defined by specifying a spatial separation between a muon and the closest jet in the  $\eta$ - $\varphi$  plane of  $\Delta R = \sqrt{(\Delta\eta)^2 + (\Delta\varphi)^2} > 0.5$ , where  $\varphi$  is the azimuthal angle. Tighter isolation is defined by requiring little tracking and calorimetric activity around the muon track.

The dominant backgrounds to  $WH$  production are from  $W +$  heavy flavor jets production, top quark pair production ( $t\bar{t}$ ), and single top quark production. Signal ( $WH$  and  $ZH$ ) and diboson processes ( $WW$ ,  $WZ$ , and  $ZZ$ ) are simulated using the PYTHIA [14] event generator and CTEQ6L [15] leading-order parton distribution functions. “ $W +$  jets” events refer to  $W$  bosons produced in association with light-flavor jets (originating from  $u$ ,  $d$ , and  $s$  quarks or gluons) or charm jets (originating from  $c$  quarks) and constitute the dominant background before  $b$ -jet identification.  $Wc\bar{c}$  and  $Wb\bar{b}$  are simulated individually and associated as “ $Wb\bar{b}$ ” for purposes of accounting. These  $W$  boson processes are generated with ALPGEN [16] interfaced to PYTHIA for showering and fragmentation, since ALPGEN provides a more complete simulation of processes with high jet multiplicities than PYTHIA. The  $t\bar{t}$  and  $Z +$  jets events are also generated using ALPGEN or PYTHIA. The production of single top quarks is simulated with COMPHEP [17].

The simulated backgrounds are normalized to their respective next-to-leading order theoretical cross sections,

with the exception of the  $W +$  jets and  $W +$  heavy-flavor samples, which are normalized to data after subtraction of all of the other backgrounds, before  $b$ -jet identification. All generated events are processed through the D0 detector simulation based on GEANT [18]. Data collected with a random bunch crossing trigger are overlaid on the simulated events to model the occupancy of the detector which is dependent on the instantaneous luminosity. The resulting events are then passed through the reconstruction software. Finally, corrections are applied to account for the trigger efficiency and for residual discrepancies between the data and the simulation.

We use a neural network  $b$ -tagging ( $NN_b$ ) algorithm [11] to identify heavy-flavor jets. Its requirements are optimized for the best sensitivity to the Higgs boson signal. For each jet multiplicity, we form two statistically independent samples, one (2  $b$ -tag) with two  $b$ -tagged jets using a loose  $NN_b$  criterion resulting in a  $b$ -jet efficiency of 59% and a light-jet tagging (mistag) probability of 1.7%, and a second (1  $b$ -tag) with exactly one  $b$ -tagged jet using a tighter  $NN_b$  criterion (48% efficiency and 0.5% mistag probability). All efficiencies are determined for jets satisfying minimum requirements in terms of track quality and multiplicity (“taggable jets”), which constitute  $\approx 80\%$  of

all jets. In the simulations, the  $b$ -tagged jets are weighted to reproduce the tagging rate measured in data samples.

Using these selection criteria, the distributions of the dijet invariant mass, using the two jets of highest  $p_T$ , are shown for the 1  $b$ -tag and 2  $b$ -tag samples of the  $W + 3$  jet events in Figs. 1(a) and 1(b). The data are well described by the sum of the simulated SM processes and multijet background. The expected contributions from a Higgs boson with  $m_H = 115$  GeV are also shown. The expected event yields for such a signal and for the backgrounds are compared to the observed number of events in Table I.

Although the dijet invariant mass is a powerful variable for separating a Higgs boson signal from background [4], the sensitivity of the analysis is enhanced through the use of multivariate techniques: In  $W + 2$  jet events, a neural network is trained on simulated signal and  $Wb\bar{b}$  events, using seven kinematic variables:  $p_T$  of the highest and second-highest  $p_T$  jets,  $\Delta R(jet_1, jet_2)$ ,  $\Delta\varphi(jet_1, jet_2)$ ,  $p_T$  (dijet system), dijet invariant mass, and  $p_T$  ( $W$  boson candidate). The training is performed for every simulated Higgs signal (different test masses) and separately for  $e$ ,  $\mu$ , 1  $b$ -tag, and 2  $b$ -tag events. The resulting neural networks are then applied to  $W + 2$  jet data and to the background and simulated signal samples. In the final limit-setting

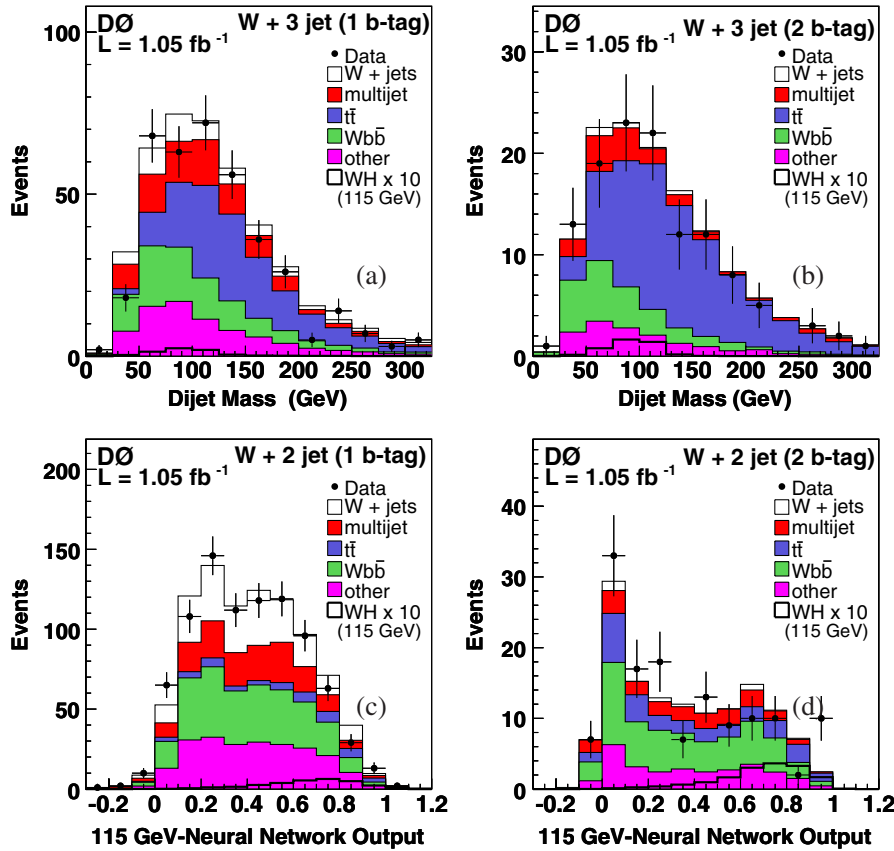


FIG. 1 (color online). Dijet mass distributions for the  $W + 3$  jet 1  $b$ -tag (a) and 2  $b$ -tag (b) events. The data are compared to the background prediction. The distributions in the neural network discriminant for  $W + 2$  jet 1  $b$ -tag and 2  $b$ -tag events are shown in (c) and (d), respectively. The expectation from  $WH(\times 10)$  production for  $m_H = 115$  GeV is overlaid.

TABLE I. Summary of event yields for the  $\ell$  ( $e$  and  $\mu$ ) +  $b$ -tagged jets +  $\not{E}_T$  final state. Events in data are compared with the expected number of 1  $b$ -tag and 2  $b$ -tag events in the  $W + 2$  and  $W + 3$  jet samples, in simulated samples of diboson (labeled “ $WZ$ ” in the table),  $W/Z + b\bar{b}$  or  $c\bar{c}$  (“ $Wb\bar{b}$ ”),  $W/Z +$  light quark jets (“ $W +$  jets”), top quark (“ $t\bar{t}$ ” and “single  $t$ ”) production, and multijet background (“ $m$  jet”) determined from data (see text). The  $WH$  expectation is given for  $m_H = 115$  GeV and not included in the “Total” SM expectation.

	$W + 2$ jet 1 $b$ -tag	$W + 2$ jet 2 $b$ -tag	$W + 3$ jet 1 $b$ -tag	$W + 3$ jet 2 $b$ -tag
$WH$	$2.8 \pm 0.3$	$1.5 \pm 0.2$	$0.7 \pm 0.1$	$0.4 \pm 0.1$
$WZ$	$34.5 \pm 3.7$	$5.3 \pm 0.6$	$9.1 \pm 1.0$	$1.7 \pm 0.2$
$Wb\bar{b}$	$268 \pm 67$	$54 \pm 14$	$87 \pm 22$	$22.7 \pm 5.7$
$W +$ jets	$347 \pm 87$	$14.0 \pm 4.4$	$96 \pm 24$	$8.5 \pm 2.7$
$t\bar{t}$	$95 \pm 17$	$37.4 \pm 7.0$	$156 \pm 29$	$81 \pm 15$
Single $t$	$49.4 \pm 9.0$	$12.4 \pm 2.3$	$15.7 \pm 2.9$	$6.7 \pm 1.2$
$m$ jet	$104 \pm 29$	$8.9 \pm 2.1$	$54 \pm 15$	$8.7 \pm 2.1$
Total	$896 \pm 177$	$132 \pm 27$	$418 \pm 76$	$129 \pm 24$
Data	885	136	385	122

procedure, the distributions of the neural network discriminant corresponding to a specific Higgs boson test mass are used for analyzing the  $W + 2$  jet events. The improvement in sensitivity over just using the dijet invariant mass is about 15% at  $m_H = 115$  GeV. The resulting neural network discriminants are shown in Figs. 1(c) and 1(d). For the  $W + 3$  jet samples, whose dominant background is  $t\bar{t}$ , the limits are determined directly from the dijet mass distributions.

Systematic uncertainties on efficiencies and from the propagation of other systematics (e.g., energy calibration and detector response) are (3–5)% for trigger efficiency, (4–5)% for lepton identification efficiency, 6% for jet identification efficiency and jet resolution, 5% from the modeling of the jet multiplicity spectrum, 3% due to the uncertainty in the jet energy calibration, 2%–10% due to the uncertainty in modeling  $W +$  jets, determined by comparing data and expectation before  $b$ -tagging and before reweighting the  $W +$  jet samples to match the data (the effect of this uncertainty on the shape of the neural network discriminant is also taken into account), 3% for jet taggability, and 2% uncertainty for  $b$ -tagging efficiency. For light quark jets, the uncertainty on the mistag rate is 15%. The multijet background, determined from data, has an uncertainty of 18%–38%. The systematic uncertainty on the theoretical cross section for the simulated backgrounds is 6%–20%, depending on the process. The uncertainty on the luminosity is 6% [19].

We use the CLs method [20,21] to assess the compatibility of data with the presence of a Higgs signal. In the absence of any significant enhancement, we obtain upper limits on  $WH$  production, using the neural network output (dijet invariant mass of the  $b\bar{b}$  system) for the  $W + 2$  jet

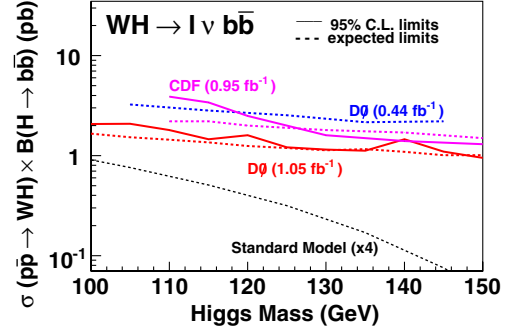


FIG. 2 (color online). 95% C.L. cross section upper limit (and corresponding expected limit) on  $\sigma(p\bar{p} \rightarrow WH) \times B(H \rightarrow b\bar{b})$  vs Higgs boson mass, compared to the SM expectation and to the expected limit from our previous analysis [4]. Recent CDF results [6] are also shown. Solid (dashed) lines represent observed (expected) limits. The contribution of  $ZH$  reconstructed in the same final state is taken into account in the  $WH$  signal when deriving the limits, assuming the SM ratio of  $ZH/WH$  cross sections.

( $W + 3$  jet) sample as the final discriminating variable. The 1  $b$ -tag and 2  $b$ -tag and the  $e$  and  $\mu$  channels are treated separately, giving a total of eight analyses, which are then combined [4]. We incorporate systematic uncertainties on signal and background expectations using Gaussian sampling and include correlations among the uncertainties across the analysis channels. The principal correlations arise from the dijet mass shape, the cross section of the backgrounds, and in the reconstruction of leptons, jets and  $b$  jets. The impact of systematic uncertainties is reduced using the profile likelihood technique which uses the data to help to constrain the backgrounds [21].

The combined upper limits obtained at the 95% C.L. on  $\sigma(p\bar{p} \rightarrow WH) \times B(H \rightarrow b\bar{b})$  are displayed in Fig. 2 and given in Table II, together with the ratios of these limits to the predicted SM cross section. For this analysis, all deviations between observed and expected limits are less than 1.5 standard deviations. At  $m_H = 115$  GeV, the observed (expected) limits are 1.5 (1.4) pb, or a factor of 11.4 (10.7) times higher than the SM prediction. Our new limits are displayed in Fig. 2 and compared to the expected limit from our previous analysis [4]. The improvement in sensitivity is significant, and our expected limits scale approximately inversely with luminosity compared to our previous result. These limits are the most stringent to date in this process at a hadron collider.

In summary, we have presented 95% C.L. upper limits on the product of  $WH \rightarrow \ell\nu b\bar{b}$  production cross section and branching fraction for  $H \rightarrow b\bar{b}$ . These range between 2.1 and 1.0 pb for  $100 < m_H < 150$  GeV, while the corresponding SM predictions range from 0.23 to 0.01 pb. The sensitivity should increase significantly in the near future with the continuing accumulation of data from the Tevatron and improvement in analysis techniques. The

TABLE II. Observed and expected 95% C.L. upper limits on the cross section times branching fraction ( $\sigma \times B$ ) in picobarns, where  $B = B(H \rightarrow b\bar{b})$ , for the Higgs boson mass values used to produce the simulated  $WH$  samples. The corresponding ratios to the predicted SM cross section are also given.

$m_H$ [GeV]	100	105	110	115	120	125	130	135	140	145	150
Exp. $\sigma \times B$	1.66	1.53	1.44	1.36	1.25	1.19	1.13	1.16	1.09	1.01	1.01
Obs. $\sigma \times B$	2.07	2.08	1.80	1.46	1.54	1.21	1.15	1.12	1.46	1.10	0.95
Exp. ratio	7.3	8.0	9.2	10.7	12.3	15.1	19.1	27.3	37.4	53.5	90.2
Obs. ratio	9.1	11.0	11.5	11.4	15.1	15.3	19.5	26.4	50.1	58.2	83.9

combination of CDF and D0 results, as in Ref. [22], has improved the overall sensitivity of Tevatron measurements; with increased integrated luminosity and further improvements in analysis under development, the Tevatron should be sensitive to a low mass SM Higgs boson.

We thank the staffs at Fermilab and collaborating institutions and acknowledge support from the DOE and NSF (USA); CEA and CNRS/IN2P3 (France); FASI, Rosatom, and RFBR (Russia); CNPq, FAPERJ, FAPESP, and FUNDUNESP (Brazil); DAE and DST (India); Colciencias (Colombia); CONACyT (Mexico); KRF and KOSEF (Korea); CONICET and UBACyT (Argentina); FOM (The Netherlands); STFC (United Kingdom); MSMT and GACR (Czech Republic); CRC Program, CFI, NSERC, and WestGrid Project (Canada); BMBF and DFG (Germany); SFI (Ireland); the Swedish Research Council (Sweden); CAS and CNSF (China); and the Alexander von Humboldt Foundation (Germany).

- [2] LEP Electroweak Working Group, <http://lepewwg.web.cern.ch/LEPEWWG/>.
- [3] V. M. Abazov *et al.* (D0 Collaboration), Phys. Rev. Lett. **94**, 091802 (2005).
- [4] V. M. Abazov *et al.* (D0 Collaboration), Phys. Lett. B **663**, 26 (2008).
- [5] D. Acosta *et al.* (CDF Collaboration), Phys. Rev. Lett. **94**, 091802 (2005).
- [6] T. Aaltonen *et al.* (CDF Collaboration), Phys. Rev. Lett. **100**, 041801 (2008).
- [7] V. M. Abazov *et al.* (D0 Collaboration), Nucl. Instrum. Methods Phys. Res., Sect. A **338**, 185 (1994).
- [8] V. M. Abazov *et al.* (D0 Collaboration), Nucl. Instrum. Methods Phys. Res., Sect. A **565**, 463 (2006).
- [9] The pseudorapidity is given in terms of the polar angle  $\theta$  as  $\eta \equiv -\ln(\tan\frac{\theta}{2})$ , where  $\theta$  is defined relative to the center of the detector.
- [10] J. Lellouch, Fermilab Report No. FERMILAB-THEESIS-2008-36, 2008.
- [11] T. Scanlon, Fermilab Report No. FERMILAB-THEESIS-2006-43, 2006.
- [12] G. Blazey *et al.*, arXiv:hep-ex/0005012.
- [13] V. M. Abazov *et al.* (D0 Collaboration), Phys. Rev. D **76**, 092007 (2007).
- [14] T. Sjöstrand *et al.*, Comput. Phys. Commun. **135**, 238 (2001); we use version 6.3.
- [15] H. L. Lai *et al.*, Phys. Rev. D **55**, 1280 (1997).
- [16] M. Mangano *et al.*, J. High Energy Phys. 07 (2003) 001.
- [17] A. Pukhov *et al.*, arXiv:hep-ph/9908288.
- [18] R. Brun and F. Carminati, CERN Program Library Long Writeup No. W5013, 1993 (unpublished).
- [19] T. Andeen *et al.*, Fermilab Report No. FERMILAB-TM-2365, 2007.
- [20] T. Junk, Nucl. Instrum. Methods Phys. Res., Sect. A **434**, 435 (1999).
- [21] W. Fisher, Fermilab Report No. FERMILAB-TM-2386-E, 2007.
- [22] The TEVNPH Working Group, for the CDF and D0 Collaborations, arXiv:0804.3423.

\*Visitor from Augustana College, Sioux Falls, SD, USA.

<sup>†</sup>Visitor from The University of Liverpool, Liverpool, United Kingdom.

<sup>‡</sup>Visitor from ECFM, Universidad Autonoma de Sinaloa, Culiacán, Mexico.

<sup>§</sup>Visitor from II. Physikalisches Institut, Georg-August-University, Göttingen, Germany.

<sup>¶</sup>Visitor from Helsinki Institute of Physics, Helsinki, Finland.

<sup>¶¶</sup>Visitor from Universität Bern, Bern, Switzerland.

<sup>\*\*</sup>Visitor from Universität Zürich, Zürich, Switzerland.

<sup>††</sup>Deceased.

[1] ALEPH, DELPHI, L3, and OPAL Collaborations, The LEP Working Group for Higgs Boson Searches, Phys. Lett. B **565**, 61 (2003).